Draft Paper for submission to 22nd International Conference on Composite Materials
Melbourne, Australia, August 2019

DEVELOPMENT OF A COMPOSITE FORMING LIMIT DIAGRAM: A FEASIBILITY STUDY

Verner Viisainen, Jin Zhou and Michael Sutcliffe

Cambridge University Engineering Department, Trumpington Street, Cambridge, CB2 1PZ, UK

Keywords: Composites, forming, non-crimp fabric, wrinkling

ABSTRACT

An experimental set-up using digital image correlation has been developed to provide data correlating non-crimp fabric (NCF) deformation with wrinkling. The strain measurements can be manipulated to find strains in critical directions, for example along the tows or in the direction of maximum compressive strain. For the NCF fabric considered here, there does not appear to be a simple correlation between the observed strains and the onset of wrinkling. Nevertheless the data provides the basis for developing a forming limit diagram. A process-specific forming limit diagram, showing the range of shear strains and blank holder forces leading to wrinkling, has been drawn up from the measurements. In conjunction with FE modelling, this could be applied in principle to different forming situations, using FE modelling to predict the corresponding variations in shear strain in these processes. This could be used to extend the applicability of forming limit diagrams derived from simple forming experiments to more complex geometries.

1 INTRODUCTION

Woven and non-crimp fabrics (NCFs) are attractive in a range of composite applications because of their good mechanical performance and handling characteristics. Typically the dry fabric will be pre-formed at low pressure, followed by a resin transfer moulding stage. Such a process route lends itself to automation with applications, for example, in the aerospace and automotive industries. However the formation of defects during draping of the fabric is a cause for concern.

Forming models for composite textiles have become reasonably mature, see for example the recent review in [1]. Wrinkling is commonly supposed to occur when the tows ‘lock-up’ as shear in the fabric reaches some critical value. However this over-simplifies the picture, with more sophisticated models and associated experiments highlighting the importance of the in-plane and bending components of the fabric forces in determining wrinkling [2,3]. More detailed material models are needed to capture the drape and wrinkling behaviour of NCFs [4,5]. While these simulations are encouraging, particularly in terms of the shear deformation modelling, the range of different modelling approaches make it difficult to define the extent of their applicability to different textile architectures and component shapes.

Given the focus on wrinkling in the literature on textile reinforcement forming, it is somewhat surprising how often, during experimental forming tests, wrinkling is only measured qualitatively and only at the end of the forming process, giving no understanding of the level of wrinkles formed or as to the development of those wrinkles. For example in [6], the wrinkling behaviour is only qualitatively observed at three different hemispherical punch displacements, and wrinkling is treated as a discrete binary behaviour with no indication of its severity. In recent years advances in imaging technology have made accurate measurement of wrinkling possible. Arnold et al [7] presented a novel, low cost method using a single camera and a shape-from-focus approach and this was successfully used to determine the wrinkle amplitudes across the entire photographed surface of the fabric blank. Digital image correlation (DIC) technology, originally developed by Sutton et al. [8], is a promising alternative. Three-dimensional digital image correlation (3D-DIC) has already been applied successfully to the measurement of out-of-plane wrinkling of a woven twill weave carbon fibre fabric during a modified bias extension test [9].

Another issue relates to the characterisation of wrinkling. Haanappel [10] introduced a forming mismatch criterion based on the difference between fabric and tool curvatures to characterise the degree of forming error. He was able to use this to show that bending, shear, and bending in conjunction with friction affected wrinkling significantly.

Strain measurement during the forming of textile reinforcements has largely focused on the measurement of the shear angle. This is because exceeding a certain critical 'locking' shear angle for the fabric can be a good predictor of wrinkling. Thus being able to measure this angle is critical to understand the fabric's formability. Again 3D-DIC provides a means to measure shear, and has been used widely, in conjunction with a speckle pattern or a grid pattern, to determine the shear angles across the surface of the fabric during forming [11].

In sheet metal forming, wrinkling and necking tend to limit the range of shapes that can be formed in a single forming operation. Here the 'forming limit diagram' has been recognised as a useful way of characterising the material behaviour, plotting the limits of forming as a function of the local strains in the material [12]. The concept is based on theoretical concepts of metal deformation, but its real value lies in the way that the forming limit diagram provides a methodology to relate a limited set of forming experiments performed with a given material to forming of complex parts using the same material.

It is the simplicity of the forming limit diagram (FLD) approach that has attracted attention in the literature towards attempting to develop a similar FLD for the forming of composites and textile reinforcements. However, due to the inherent anisotropy and the indeterminate failure point (for textile reinforcements) of these materials, it makes such a diagram much more challenging to generate. The concept of a FLD for composites has been explored in [13] in the context of material shear deformation and applied to thermoplastic sheet forming by Wolthuizen et al [14]. Two of the pioneers of applying FLDs to composites were Dessenger and Tucker, who proposed an experimental method [15] and an FE model [16] for determining the failure limits of random-fibre mat composites in terms of the major and minor stretch ratios. However, their approach assumed that random fibre mats behave isotropically and thus it cannot be applied to textile reinforcements or continuous fibre composites. One of the earliest attempts for textile composites was made by Zhu et al. [17], who represented the wrinkling limits of a woven glass fibre reinforced polypropylene preform in terms of its material properties, critical shear angle and two factors related to the mould shape and blank sheet orientation. The critical values were predicted using a bespoke analytical model for the onset of wrinkling based on energy balance considerations [17]. Experimental attempts at the FLD soon followed with Vanclooster et al. [18] proposing FLD for multi-layer forming in terms of the critical shear angle and the relative orientation between layers based on experimental data. Wang et al. [19] used a 3D-DIC approach to measure the surface strains at failure for a range of hour glass samples of different widths made from flax reinforced polypropylene, which were then post-processed to generate a forming limit diagram in terms of the fibre strain and strain ratio. A similar study by Zanjani et al. [20] showed that the FLD for a self-reinforced polypropylene varied significantly based on the orientations of the fibres in the composite, using a 'cloud plot' approach of plotting all the surface strains to visualise the fabric conditions at failure.

Although the studies described above have applied the FLD method to composites forming, the approach has not been applied in a way that can be used to predict wrinkling in general forming processes for textile composites. The hypothesis of this feasibility study is that the forming limit diagram concept can be extended to define the limits on forming to avoid defects typically found in composite textiles forming. A key step in testing this hypothesis is development of a complete set of data on fabric strains and wrinkle amplitudes, as described in section 2 of this paper. Section 3 shows how this data can be applied to development of a forming limit diagram. Section 4 describes a modelling approach which can be used to help with application of the model.

2 FORMING EXPERIMENTS

The aim of the forming experiments is to provide detailed data on wrinkling and fabric deformation in order to be able to construct an appropriate forming limit diagram. The hypothesis is that compressive straining would be associated with wrinkling/buckling, and measurement of strain in different directions could be used to assess the build-up of such compressive strains.

2.1 Material

The material used for this study was a biaxial ±45° NCF fabric (supplied by Hexcel, material code FCIM359). The fabric was made from 24k carbon tows with texturised polyester pillar stitching and an areal weight of 441 gsm.

2.2 Forming methodology

The experimental methodology for wrinkle measurement was based on the forming study of Arnold et al. [7]. The general dimensions and geometry of the forming set-up were kept the same, with a hemispherical punch of radius 75 mm deforming a circular blank of fabric, which was constrained by a blank holder ring. Loading on the weight ring was used to regulate the blank holder force. The new system is shown in Fig. 1, illustrating several improvements, including the addition of a linear actuator to drive the punch and an ARAMIS 3D-DIC system to replace the single camera in the original set-up. The 3D-DIC system is essential because it not only allows the deformation of the NCF blank to be tracked and therefore the wrinkling development to be characterised, but it also allows the surface strains on the fabric to be determined. A bespoke control algorithm was written in the Labview environment to control the rig actuation and punch load sampling.

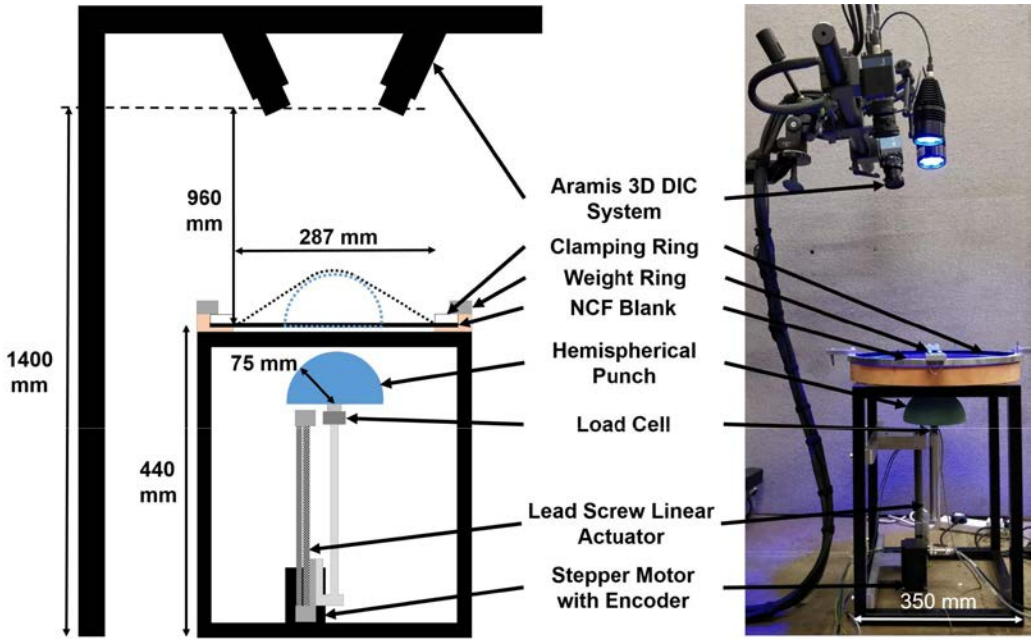

Fig. 1. Schematic (left) and photograph (right) of the experimental forming setup

2.3 DIC measurements

For a DIC system to work correctly, the surface of the material needs to be treated with a pattern that will allow the system to identify unique facet points between frames [8]. Most commonly, for non-porous objects such as steel, this is done by spraying the surface of the material with a speckle pattern using black and white matte spray paint, with one paint being used to create a uniform base layer onto which the speckle dots are sprayed with the other colour. However, because of the porous nature of NCF, paint was not suitable because it would seep into the fabric and thus significantly affect its deformation properties (especially bending stiffness). A range of potential materials were sprayed or applied onto a sample of NCF and then the pattern clarity and effect on the fabric were evaluated. A suitable pattern method was identified as using graphite spray "Kontakt Chemie Graphit 33" as the base layer and a white flaw detector spray "Ambersil Flaw Detector Developer 3" for the top layer of speckles.

2.4 Wrinkle characterisation

While the ARAMIS 3D-DIC system and software provides maps of displacements during the deformation process, a significant amount of post processing is required in order to convert this data into the wrinkle amplitudes and fibre strains required. The post processing was implemented in Matlab. The wrinkle amplitude is calculated by taking the difference between the out-of-plane Z displacement of the fabric and a smoothed out Z displacement, following [7], to give a surface map highlighting the amplitudes and locations of the fabric wrinkles. Figure 2 illustrates the extraction of the wrinkle

amplitude from the raw measured displacement. The smoothed wrinkle amplitude, Fig. 2(d), is used to characterise the average absolute wrinkle magnitude in regions where there are several closely spaced wrinkles of both positive and negative amplitudes.

The effect of blank holder force on wrinkling is shown in Fig. 3, illustrating how, for the forming diameter of 287 mm, an increase in blank holder force reduces the wrinkle amplitude significantly. This result, matching previous findings [7], confirms the need for a predictive model for wrinkling which can take into account membrane stresses and constraints, rather than adopting a purely kinematic approach.

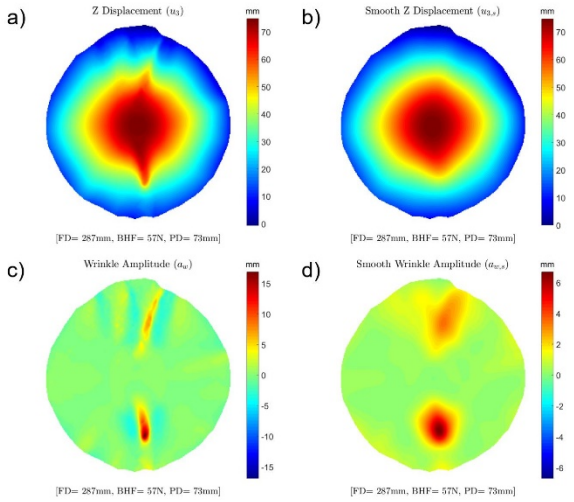

Fig. 2. Determining the wrinkle amplitude: (a) *Z* displacement of the fabric, b) smoothed out *Z* displacement, (c) wrinkle amplitude = (a)-(b), (d) smoothed wrinkle amplitude.

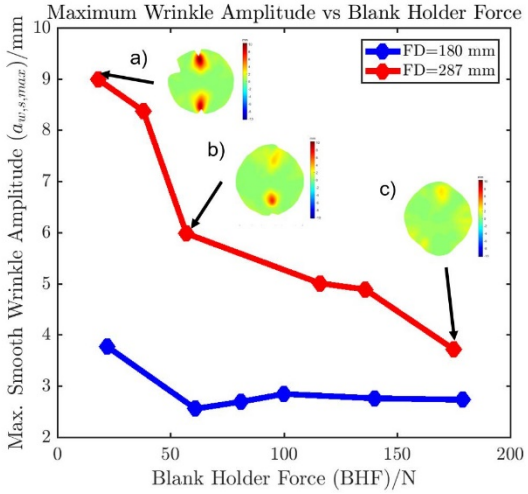

Fig. 3. The variation of maximum smooth wrinkling amplitude with blank holder force, for forming diameters of 180 mm and 287 mm.

2.5 Extraction of strains

The ARAMIS 3D-DIC system takes images using both its cameras at a constant frequency. The corresponding ARAMIS Professional software uses those images in conjunction with the reference image to determine the deformation gradient, *F*, across the fabric surface at all time steps. This deformation gradient is then decomposed, via polar decomposition, into the rotation tensor, *R*, and the stretch tensor, *U* [21]:

$$F = R \cdot U \tag{1}$$

The components of the stretch tensor U are directly used to compute the normal strains, ε_x and ε_y, and the shear strain, ε_{xy}, in the global coordinate system *XYZ*, as follows [21]:

$$U = \begin{pmatrix} \varepsilon_x + 1 & \varepsilon_{xy} \\ \varepsilon_{xy} & \varepsilon_{xy} + 1 \end{pmatrix} \tag{2}$$

The obtained strains are then used to determine the eigenvalues, λ_1 and λ_2, which directly correspond to the major and minor strains (ε_1, ε_2) by [21]:

$$\lambda_{1,2} = 1 + \frac{\varepsilon_x + \varepsilon_y}{2} \pm \sqrt{\left(\frac{\varepsilon_x - \varepsilon_y}{2}\right)^2 + \varepsilon_{xy}^2} = \varepsilon_{1,2} + 1 \tag{3}$$

The corresponding eigenvectors, v_1, v_2, are calculated by substituting each eigenvalue into the following equation containing the 3D stretch tensor, *U*, and solving for *v*:

$$\left(U - \lambda_{1,2}\right) \cdot v_{1,2} = 0 \tag{4}$$

These eigenvalues are direction vectors with components in the global *X*, *Y* and *Z* directions, representing the respective directions of the major and minor strains. Standard rotation matrices are then used to derive the strains in arbitrary directions, including along the tow directions or in the radial and circumferential directions.

Figure 4 illustrates typical results from the forming experiments for the strain distribution along and transverse to the fibre directions, and the corresponding shear angle. Results show that the shear angle is reliably measured with regions of large positive shear developing in the North and South regions with the rest of the fabric in slight negative shear. This shear behaviour can be explained by stitching in the fabric that prevents shearing in one direction but not the other. However, although fibre and transverse strains can be reasonably well captured, the results do not exhibit any clear strain pattern with significant amounts of scatter across the fabric. The small magnitude of these strains would also seem to indicate they are not as significant as the shear behaviour.

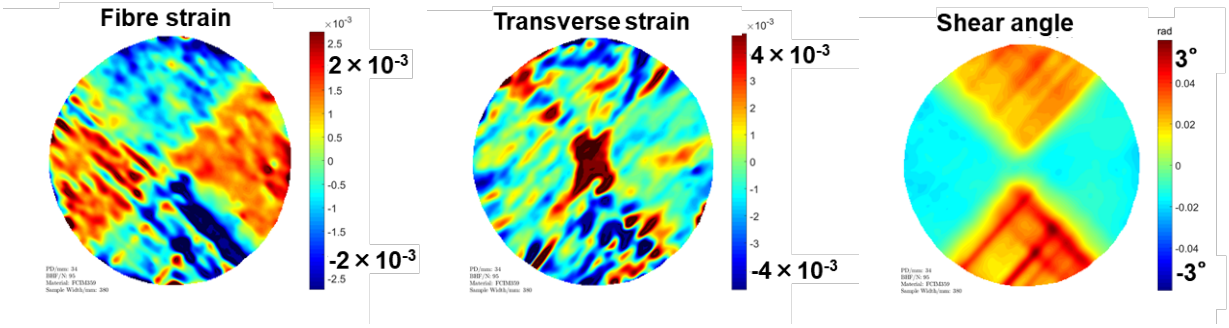

Fig. 4. The variation across the blank of: (a) fibre strain, (b) transverse strain and (c) shear angle at a punch displacement of 34 mm with a forming diameter of 287 mm and a blank holder force of 95 N. The stitch (0°) direction runs horizontally.

3 FORMING LIMIT ANALYSIS

It is expected that wrinkling is the result of compressive stresses arising in the fabric. Figure 5 shows the correlation of shear angle and circumferential strain with wrinkle amplitude for a given forming test. Regions of high shear and relatively large compressive strains in the North and South quadrants are indeed locations where wrinkles are present. But in addition there is a correlation between wrinkling and the regions of compressive straining in the West and East regions. This result illustrates the challenge in developing failure criteria, with mixtures of deformation leading to wrinkling. Nevertheless it is very encouraging that the experimental approach is able to provide the key information required to link deformation with wrinkling.

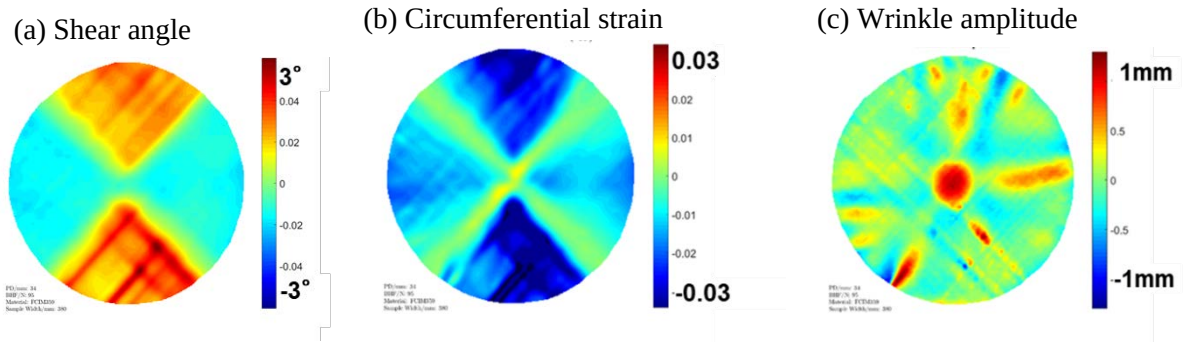

Fig. 5. Correlation of (a) shear angle and (b) circumferential strain with (c) wrinkle amplitude for a punch displacement of 34 mm, with a forming diameter of 287 mm and a blank holder force of 95 N.

The variation of wrinkle amplitude with punch deformation and corresponding shear strain is used in Fig. 6 (a) to define the point at which a critical wrinkle amplitude of 1 mm is exceeded. Using the results with different blank holder forces, a process-specific forming limit diagram can then be drawn up, showing the combination of blank-holder force and shear angle which leads to wrinkling. In principle the shear angle can be predicted from a finite element calculation for different geometries (see the following section), allowing this approach to be used to apply the wrinkling results for the simple hemispherical punch to other geometries and blank holder configurations, taking into account the material deformation properties and fabric membrane tensions developed.

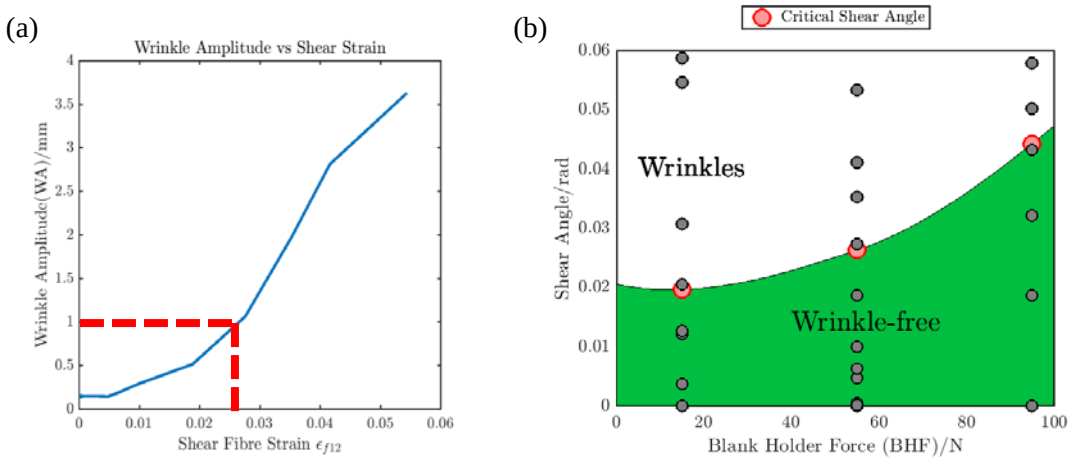

Fig. 6. A process-specific forming limit diagram for a forming diameter of 287 mm: (a) identification of critical shear angle at onset of wrinkling, (b) combination of shear angle and blank holder force giving wrinkling.

4 DEFORMATION MODELLING

As noted in the introduction, there have been a number of numerical modelling approaches aimed to predict wrinkling in fabrics *a priori*. The aim of the modelling work developed here is not to provide such a predictive capability, which requires sophisticated material models for each fabric. Rather the goal is to support the experimental forming limit diagram approach. A suite of experimental tests provides a failure or wrinkling criterion, with the model used to predict whether the failure criterion will be exceeded during a specific forming process. To perform such a role, the model needs only to be able to predict the strains and stresses arising from the deformation, rather than directly predicting wrinkles.

A numerical model was developed in Abaqus/Explicit replicating the forming geometry, including the blank holder configuration, as illustrated in Fig. 7. A constant blank holder force of 175 N was used with a coefficient of friction on the fabric of 0.4. The fabric was modelled using the phenomenological Abaqus *Fabric material model, with input data taken from [6] and in-house tests. This is a non-linear anisotropic behavior with two fibre orientations. The fabric was modelled using membrane elements (M3D4R) with a mesh size of side-length 3-5mm.

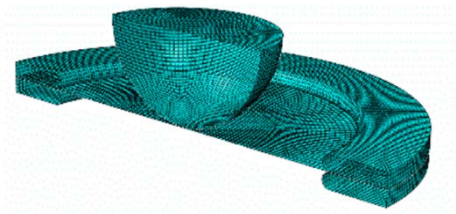

Fig. 7. FE model of forming process.

Figure 8 compares the predictions of the shear angle distribution with measured values, for a punch holder displacement of 17 mm. The corresponding variation of maximum shear angle with punch displacement is given in Fig. 9. Agreement is good, suggesting that the model is adequately able to capture the shear deformation response. Further work is needed to assess the direct strain capabilities of the model.

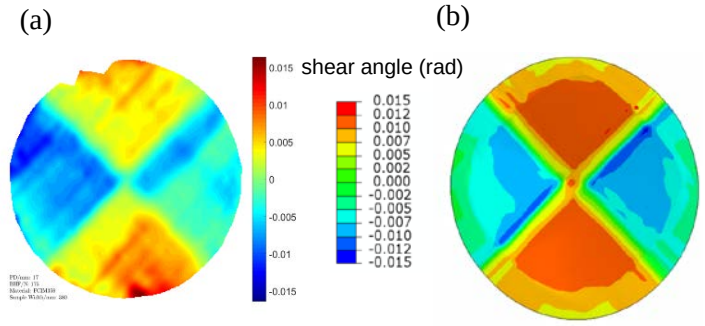

Fig. 8. Comparison of (a) experimental and (b) predicted shear angle distributions, at a punch displacement of 17 mm.

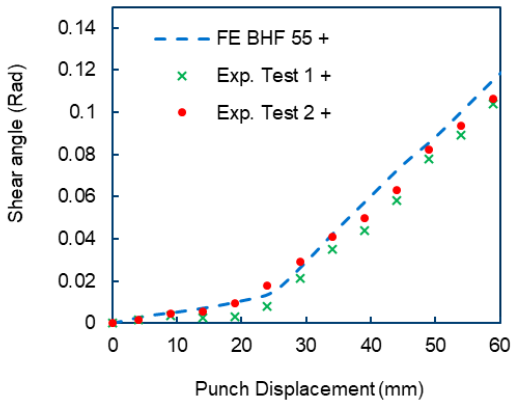

Fig. 9. Comparison of experimental and predicted variation of maximum shear angle with punch displacement.

5 CONCLUDING DISCUSSION

The feasibility study described in this paper has demonstrated that an experimental set-up using DIC is able to provide data correlating fabric deformation with wrinkling. The strain measurements can be manipulated to find strains in critical directions, for example along the tows or in the direction of maximum compressive strain. For the NCF fabric considered here, there does not appear to be a simple correlation between the observed strains and the onset of wrinkling. Presumably the architecture of the fabric in its deformed state determines where and when wrinkling occurs. While the experimental work provides the tools to explore that, it is suggested that meso-scale architecture-based FE modelling, taking advantage of Texgen modelling capability [22], linked to these experiments will be needed to guide a wrinkling criterion which can be used in conjunction with these measurements.

A process-specific forming limit diagram, showing the range of shear strains and blank holder forces leading to wrinkling, has been drawn up from the measurements. In conjunction with FE modelling, this could be applied in principle to different forming, using FE modelling to predict the corresponding variations in shear strain in these processes. While a proposed FE approach gives acceptable predictions of shear strain in the experiments undertaken here, further validation is required both of the FE predictions for compressive strains, and for a wider range of deformations in order to demonstrate the accuracy of this approach.

In summary the proposed hybrid approach, of using experimental characterisation in conjunction with a simple FE model, shows considerable promise as a way of defining the forming limits for composite fabrics. Further work is needed, particularly on extending the range of deformation processes and understanding better the link between changes in tow architecture and wrinkling.

ACKNOWLEDGEMENTS

The authors are pleased to acknowledge the advice and practical assistance from John Klintworth (Dassault Systèmes), Dimitris Karanatsis (Hexcel), Lee Harper, Shuai Chen and Nick Warrior (University of Nottingham). The financial support of the EPSRC via the CIMComp Future Composites Manufacturing Research Hub (Grant reference EP/P006701/1) is gratefully acknowledged.

REFERENCES

1. T. Gereke, D. Döbrich, M. Hübner and C. Cherif “Experimental and computational composite textile reinforcement forming: A review”. *Composites Part A: Applied Science and Manufacturing*, Vol. 46, pp 1-10, 2013.

2. S. Allaoui, P. Boisse, S. Chatel, et al. “Experimental and numerical analyses of textile reinforcement forming of a tetrahedral shape”. *Composites Part: Applied Science and Manufacturing* ,Vol. 42, pp 612–622, 2011.

3. J. Pazmino, V. Carvelli, and S V. Lomov “Formability of a non-crimp 3D orthogonal weave E-glass composite reinforcement”. *Composites Part A: Applied Science and Manufacturing*, Vol. 61, pp76–83, 2014.

4. S. Bel, P. Boisse and F. Dumont “Analyses of the deformation mechanisms of non-crimp fabric composite reinforcements during preforming”. *Appl Compos Mater*, Vol. 19, pp513–528, 2012.

5. W.R. Yu, P. Harrison, and A. Long “Finite element forming simulation for non-crimp fabrics using a non-orthogonal constitutive equation”. *Composites: Part A: Applied Science and Manufacturing*, Vol.36, pp1079–1093, 2005.

6. S. Chen, O.P.L. McGregor, L.T. Harper, A. Endruweit, and N.A.Warrior “Defect formation during preforming of a bi-axial non-crimp fabric with a pillar stitch pattern”. *Composites Part A: Applied Science and Manufacturing*, Vol. 91, pp156–167, 2016.

7. S. Arnold, M.P.F. Sutcliffe, W.L.A. Oram “Experimental measurement of wrinkle formation during draping of non-crimp fabric”. *Composites Part A: Applied Science and Manufacturing*, Vol. 82, pp159-169, 2016.

8. M.A. Sutton, J.J. Orteu, H.W. Schreier. “Image Correlation for Shape, Motion and Deformation Measurements: Basic Concepts,Theory and Applications”. *Springer Publishing Company*, New York City, 1st edition, 2009.

9. P. Harrison, M.F. Alvarez and D. Anderson. “Towards comprehensive characterisation and modelling of the forming and wrinkling mechanics of engineering fabrics”. International *Journal of Solids and Structures*, Vol. 0, pp1–17, 2017.

10. S.Haanappel, “Forming of UD fibre reinforced thermoplastics: a critical evaluation of intra-ply shear”. PhD Thesis, University of Twente, Netherlands, 2013.

11. S.V. Lomov, P. Boisse, E. Deluycker, F. Morestin, K. Vanclooster, D. Vandepitte, I. Verpoest and A. Willems. “Full-field strain measurements in textile deformability studies”. Composites Part A: Applied Science and Manufacturing, Vol. 39, No. 8, pp1232–1244, 2008.

12. Z. Marciniak, J.L. Duncan, S.J. Hu “Mechanics of sheet metal forming”. Butterworth-Heinemann. p. 75, 2002.

13. A.S. Tam and T.G. Gutowski, “The kinematics for forming ideal aligned fibre composites into complex shapes”. *Composites Manufacturing*, Vol 1, pp219-228, 1990.

14. D. J. Wolthuizen,, J. Schuurman, and R. Akkerman “Forming limits of thermoplastic composites”. *Key Engineering Materials*, Vols. 611-612, pp. 407-414, 2014.

15. R.B. Dessenberger and C.L. Tucker Forming limit measurements for random-fiber mats. *Polymer Composites*, Vol. 19 No. 4, pp 370–376, 1998.

16. Dessenberger RB, Tucker CL. Ideal Forming Analysis for Random Fiber Preforms. *Journal of Manufacturing Science and Engineering*, 125(1):146, 2003.

17. B, Zhu, T.X. Yu, H. Zhang and X.M. Tao. “Experimental investigation of formability of woven textile composite preform in stamping operation”. *International Journal of Material Forming*, 1(SUPPL. 1) pp 969–972, 2008.

18. K. Vanclooster, S.V. Lomov and I.Verpoest “On the formability of multi-layered fabric composites”. *Proceedings of the 17th International Conference on Composite Materials*, pp 1–10, 2009.

19. W. Wang, A. Lowe, A. Davey, N.A. Zanjani and S. Kalyanasundaram. “Establishing a new Forming Limit Curve for a flax fibre reinforced polypropylene composite through stretch forming experiments”. *Composites Part A: Applied Science and Manufacturing*, Vol. 77, pp114–123, 2015.

20. N.A. Zanjani, S. Kalyanasundaram, “A comparison between forming behaviours of two pre-consolidated woven thermoplastic composites”. *Journal of Materials Science and Chemical Engineering*, Vol. 3 pp:180–189, 2015.

21. GOM GmbH. “Digital Image Correlation and Strain Computation Basics”. *Technical report, Braunschweig*, 2016.

22. Texgen.sourceforge.net, 2017.